

Article

## Integrating Quickbird Multi-Spectral Satellite and Field Data: Mapping Bathymetry, Seagrass Cover, Seagrass Species and Change in Moreton Bay, Australia in 2004 and 2007

Mitchell Lyons \*, Stuart Phinn and Chris Roelfsema

Biophysical Remote Sensing Group, Centre for Spatial Environmental Research, School of Geography, Planning and Environmental Management, University of Queensland, Brisbane, QLD 4072, Australia; E-Mails: s.phinn@uq.edu.au (S.P.); c.roelfsema@uq.edu.au (C.R.)

\* Author to whom correspondence should be addressed; E-Mail: m.lyons@uq.edu.au; Tel.: +61-7-3346-7023; Fax: +61-7-3365-6899.

Received: 28 October 2010; in revised form: 24 December 2010 / Accepted: 31 December 2010 / Published: 6 January 2011

---

**Abstract:** Shallow coastal ecosystems are the interface between the terrestrial and marine environment. The physical and biological composition and distribution of benthic habitats within these ecosystems determines their contribution to ecosystem services and biodiversity as well as their connections to neighbouring terrestrial and marine ecosystem processes. The capacity to accurately and consistently map and monitor these benthic habitats is critical to developing and implementing management applications. This paper presents a method for integrating field survey data and high spatial resolution, multi-spectral satellite image data to map bathymetry and seagrass in shallow coastal waters. Using Quickbird 2 satellite images from 2004 and 2007, acoustic field survey data were used to map bathymetry using a linear and ratio algorithm method; benthic survey field data were used to calibrate and validate classifications of seagrass percentage cover and seagrass species composition; and a change detection analysis of seagrass cover was performed. The bathymetry mapping showed that only the linear algorithm could effectively and accurately predict water depth; overall benthic map accuracies ranged from 57–95%; and the change detection produced a reliable change map and showed a net decrease in seagrass cover levels, but the majority of the study area showed no change in seagrass cover level. This study demonstrates that multiple spatial products (bathymetry, seagrass and change maps) can be produced from single satellite images and a concurrent field survey dataset. Moreover, the products were produced at higher spatial resolution and accuracy levels than previous studies in Moreton Bay. The methods are developed from

previous work in the study area and are continuing to be implemented, as well as being developed to be repeatable in similar shallow coastal water environments.

**Keywords:** remote sensing; bathymetry; seagrass; change detection; Quickbird; high resolution

---

## 1. Introduction

Seagrass communities are vital contributors to ecosystem services and biodiversity in shallow coastal areas [1]. The spatial distribution of seagrass beds determines their effectiveness as ecosystem stabilisers, thus disturbances to seagrass, in particular habitat fragmentation, can effect the entire coastal ecosystem [2]. The dynamics of long term change in spatial distribution of seagrass communities are largely unknown, stemming from the lack of understanding in short-term change in spatial patterns [3].

Seagrass mapping can be approached in different ways and methods vary depending on output requirements and site conditions [4]. Spatial and categorical mapping resolution can range from moderate (e.g., Landsat Thematic Mapper) to high (e.g., Quickbird) and the imaging sensor can be airborne or satellite based [5-9]. Seagrass mapping is generally performed to derive three main biophysical properties: seagrass cover or projected foliage cover; seagrass species composition and seagrass biomass [10]. Higher spatial resolution image data increases both the accuracy and precision of image classification and modelling [11] and is a prerequisite for delineating species composition of seagrass patches [12].

Remote sensing is useful for monitoring shallow coastal ecosystems with clear water, due to good light penetration and easily accessible field data [4]. Moreover, remote sensing has been shown to be more cost-effective than field survey data collection in some situations [13] and should be considered as an integral approach along with field survey for monitoring seagrass communities. Mapping seagrasses via remote sensing can produce a more spatially comprehensive and inclusive representation of spatial distribution than point or transect based surveys. Only recently, in Moreton Bay, have the first studies mapping wide spread spatial distribution of several seagrass attributes been completed [8,9], with previous studies [14-16] focusing on relatively limited areas or physical attributes. Bathymetric structure is essential to understanding aquatic system geomorphology and modelling system dynamics [17] as well as being an important factor in determining seagrass distribution. Bathymetry (*i.e.*, water depth and light penetration limit) is a physical limitation for seagrass growth [1] and is fundamental in controlling the associated ecosystem productivity. Incorporation of bathymetric data can also significantly increase mapping accuracy of seagrass [6,18] and is essential in benthic habitat modelling. The aim of this work is to produce both benthic cover and bathymetry products from single image data sets for use by scientists and managers.

Bathymetry mapping was performed by applying both a linear and ratio empirical algorithm to 2004 and 2007 Quickbird satellite image data, using known depths (field survey transects) to calibrate and assess accuracy of the outputs. Two different methods were explored for extracting water depth from the image data. A reflectance ratio based algorithm developed by [19] and a linear algorithm

developed by [20] and [21]. Using these algorithms, water depth was derived from the image data and was assessed for accuracy against known depths from field survey transects. This study also produced both seagrass percentage cover and species composition maps. Seagrass cover was classified in four discrete cover classes (0–10, 10–40, 40–70, 70–100%) and seagrass species composition by mono-specific and dominant species combination classes. Both Quickbird images were classified using a field photo method that integrates field data/photos into a supervised classification process. GPS linked benthic photos were analysed to create seagrass cover and species composition datasets and then used to extract spectral signatures to train classifications. The accuracy assessment of the seagrass maps is based on the remaining field photos/data, not used for the classification process [8,9]. Finally a change detection analysis was performed to quantify the amount of change in seagrass cover distribution between 2004 and 2007. This was done via a post classification comparison; producing (1) a change matrix that will quantify (per pixel) class changes from 2004 to 2007 and (2) a corresponding image showing these changes visually as a map.

## 2. Methods

### 2.1. Study Site

This study is an integrated mapping approach for mapping bathymetry and seagrass and assessing its change in the Eastern Banks, Moreton Bay. The Eastern Banks is a seagrass dominated region, approximately 200 km<sup>2</sup>, to the west of North Stradbroke Island, Australia (Figure 1). This site was chosen primarily due to familiarity and access to previous research in the area involving the authors. This site is particularly suitable to a remote sensing project due to the optically clear waters and easy accessibility for field work.

### 2.2. Image Data Acquisition

The image data used for this study included three Quickbird-2 satellite images obtained from the Centre for Remote Sensing and Spatial Information Science (CRSSIS), University of Queensland. Two Quickbird multi-spectral 2.44 m pixel (blue, green, red, infrared bands) images were acquired on 17 September 2004 and 4 July 2007. The images were atmospherically corrected to at-surface reflectance using the ITT ENVI 4.5 FLAASH module (Mid-Latitude Winter Atmos. Model; Maritime Aerosol Model). For the 4 July 2007 image acquisition, a 0.64 m pan-sharpened multi-spectral (blue, green, red) image was created with the corresponding pan-chromatic band, using the Gram-Schmidt Spectral Sharpening tool in ITT ENVI 4.5. The pan-sharpened image was only used for georeferencing operations (detailed section 2.4); all bathymetry and seagrass processing and analyses was performed on the 2.44 m multi-spectral images. The 2007 image was captured at a tidal stage approximately 0.6 m lower than the 2004 image but it was decided that relative to the temporal variances in the field data, the factor of tidal stage could not be appropriately accounted for in this study. Table 1 shows the summarised image details for the two Quickbird images.

**Figure 1.** The Eastern Banks, Moreton Bay and a 1 km × 1 km area zoomed on the Wanga Wallen Banks (inset). The 2004 (red) and 2007 (green) seagrass field survey data is overlaid. 6 major areas are labelled; (1) Moreton Island, (2) Moreton Banks, (3) Maroom Banks, (4) Amity Banks, (5) Wanga Wallen Banks, (6) N<sup>th</sup> Stradbroke Island. Image data–Quickbird, true colour, BGR bands, 2.4 m pixels, 4 July 2007) (Image source and copyright: DigitalGlobe).

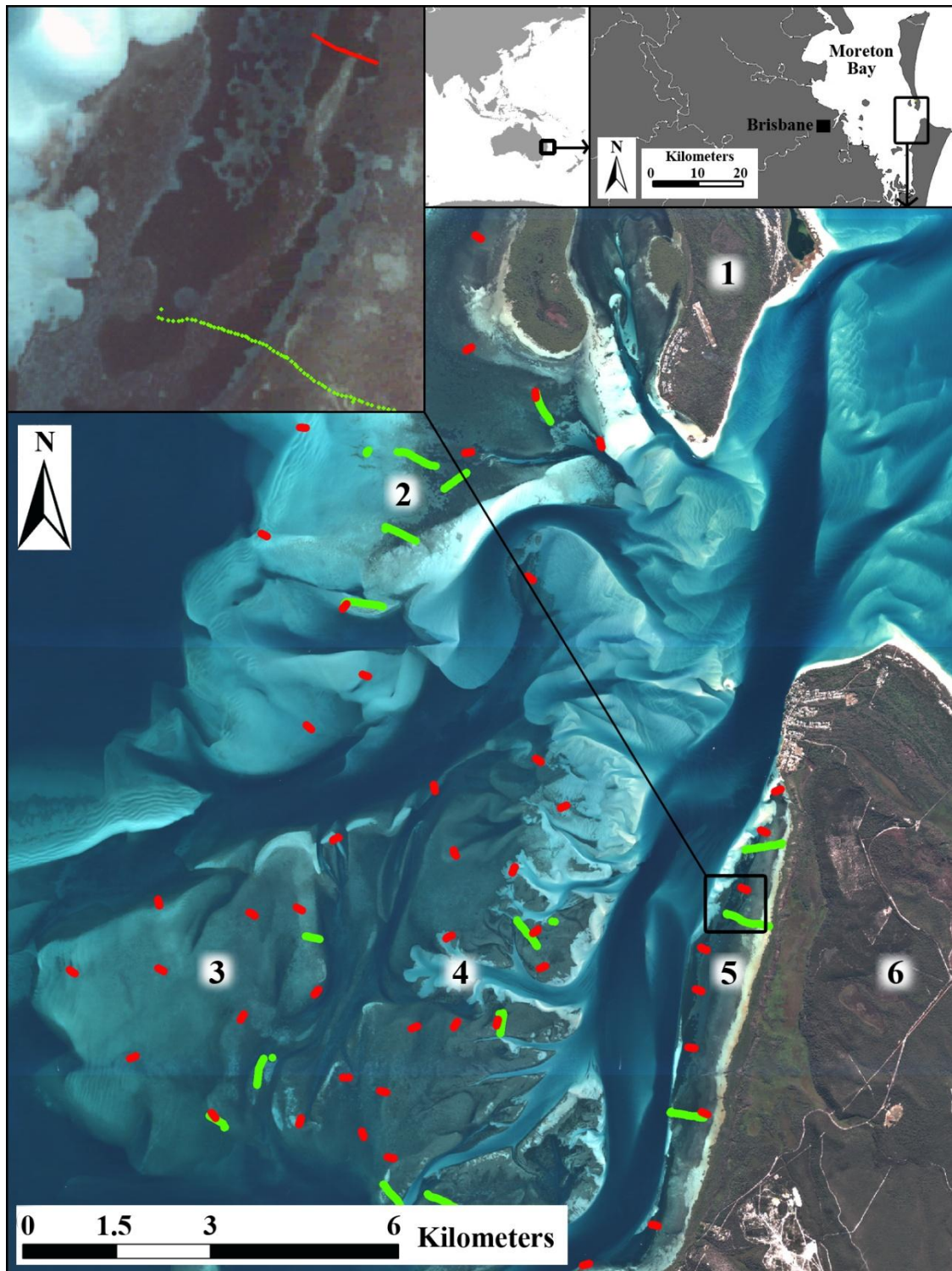


**Table 1.** Detailed information for the 2004 and 2007 Quickbird image data sets including tidal stage. Brisbane Bar tide information was converted using the Amity Point offset from the NTT semidiurnal tidal plane and the tidal stage was estimated using the NTT standard tidal curve, at a tidal range of 1.0 m.

Quickbird-2	2004	2007
Date Acquired	17 September 2004	4 July 2007
Time Acquired	0950 local	1012 local
Source	Digital Globe	Digital Globe
Tidal Stage-adjusted for Amity Point	Approximately 1.7 m at 0950 High tide: 1.73 m at 1016 local	Approximately 1.1 m at 1015 Low tide: 0.36 m at 0516 High tide: 1.42 m at 1112
Pixel Size	2.4 m (multispectral)	2.4 m (multispectral); 0.64 m (pan-sharpened)
Band Ranges	<b>Blue:</b> 0.45–0.52 $\mu\text{m}$ <b>Green:</b> 0.52–0.60 $\mu\text{m}$ <b>Red:</b> 0.63–0.69 $\mu\text{m}$ <b>NIR:</b> 0.76–0.90 $\mu\text{m}$	<b>Blue:</b> 0.45–0.52 $\mu\text{m}$ <b>Green:</b> 0.52–0.60 $\mu\text{m}$ <b>Red:</b> 0.63–0.69 $\mu\text{m}$ <b>NIR:</b> 0.76–0.90 $\mu\text{m}$

### 2.3. Bathymetry and Seagrass Data Acquisition and Analysis

Field data used in the bathymetry mapping and seagrass mapping processing was obtained from previous research [8,9]. Bathymetry data was collected using a depth sounder on board a boat, within approximately two months of image acquisition. Depth measurements were linked to GPS measurements from an onboard, automatically logging Garmin GPS unit and compiled into point vector files. Several thousand depth measurements were collected over the 2004 and 2007 surveys. The benthic field data included multiple transect surveys for 2004 and 2007 (close to the image capture dates), which were conducted using a standardised field survey approach developed in [8,9,22], across the entire Eastern Banks region. For the seagrass field data, a snorkeler would take a series of digital photos of the benthic cover approximately 1 m above the bottom, creating photos approximately 1 m  $\times$  1 m at approximately 2–3 m intervals. The initial transects in 2004 were collected along a 100 m long measurement tape. The survey technique was refined for 2007; no measurement tape was used and a GPS unit was attached to the snorkeler to allow coverage over larger survey areas. As a result the transects in 2007 varied in length. The snorkeler towed an automatically logging Garmin GPS unit, sealed in a dry bag on the surface, so each photo could be spatially referenced to the image data. Several thousand photos were captured for both 2004 and 2007. The photos were subsequently analysed by placing a 24 point grid on each photo, with each point being evaluated for seagrass species or bottom cover type (e.g., algae/sand/mud). Seagrass cover was calculated as a percentage of the number of points in the photographed area where seagrass was present (24 points =  $\pm 5\%$  accuracy).

### 2.4. Image Georeferencing

The multi-spectral and pan-chromatic images, were obtained as standard Quickbird products (registration  $\pm 3.0$  m). The pan-sharpened image was used in conjunction with a field survey, to

increase georeferencing accuracy of the images. GPS data were collected for 29 control points around the Eastern Banks and North Stradbroke Island using a GPS unit with a differential receiver, recording a 60 second average at each site. The differential receiver increases the accuracy of the measurements to 2–5 m. Marine control points were navigation markers distributed throughout the Eastern Banks and visible on the 2007 multi-spectral and pan-sharpened multi-spectral images. The Eastern Banks control points were recorded by holding the GPS unit against the navigation markers. The land based control points were features (e.g., road line markings that were visible on the 2007 pan-sharpened image, such as road lines, helicopter pad, jetty pylons and small buildings). The land based control points were recorded by standing directly over the feature with the GPS unit. Many of the control point features were also visible on the 2007 and 2004 multi-spectral images. The DGPS field data were used as a reference to rectify the 2007 pan-sharpened image, reducing the error associated with GPS registered field data. The 2007 and 2004 multi-spectral images were corrected to within one pixel using the 2007 pan-sharpened image as a reference.

### 2.5. Image Masking

To ensure the suitability of the images for the bathymetry and seagrass mapping procedures, some sections of the images were masked out. For the bathymetry mapping procedure, only a simple land/water mask was required. For the seagrass mapping procedures, in addition to the exposed features, all areas below 3.0 m deep were also masked out. [8,9,23,24] have shown that mapping seagrass cover and seagrass species composition with multi-spectral data can only be reliably achieved in water depths of 3.0 m or less in Eastern Moreton Bay waters. The majority of the seagrass over the Eastern Banks is in waters less than 3.0 m.

### 2.6. Bathymetry Mapping

The data from the two multi-spectral images were first examined to explore the relationship between observed reflectance and water depth. The bathymetry field data was used to select training sites of specific cover and albedo at known depths. These training sites included sand and low/high albedo seagrass at depths ranging from 0 to 20 m. These data were then imported into spreadsheets where reflectance values in separate bands were compared against each other and known depths. The results from this exploration were used to guide the algorithm application and are presented in the results section.

#### 2.6.1. Linear (Lyzenga) Algorithm

The Lyzenga algorithm used in this study has been shown to be able to accurately derive water depth in many different environments [6,18-20,25]. The main argument against using a Lyzenga algorithm is that it cannot account for varying albedo (*i.e.*, it does not work, without extensive tuning/calibration, over areas with a variety of benthic cover types) [6,19]. As such, the use of this algorithm was confined to uniform substrate by separating the image into substrate type and separately applying the algorithm. Plotting the log transform of observed reflectance variation over a range of depths and fitting a line to the data produces multiple straight lines, where each one represents a

different bottom type. For each of these lines the depth ( $Z$ ) can be calculated [20,21,26] according to the following equation (Equation 1):

$$Z = a + \sum_{i=1}^3 b X_i \quad (1)$$

$X_i$  is the log transform of observed reflectance for bands 1, 2 and 3 (blue, green and red). A regression analysis was performed on the log transformed reflectance values in the green band, occurring within a uniform substrate type. Only the green band was used due to inhibitory levels of scattering and attenuation in the blue and red bands respectively [25]. Thus, equation 1 is no longer a summation; it becomes a single linear equation for the green band. Pixels were chosen where depth is known from field data, calibrating the equation so it may be used on the whole cover type. The algorithm was applied to separate cover type by simply creating separate seagrass and sand layers from the image via an unsupervised classification and subsequent masking procedures. A map of water depth (in metres) was created for both the 2004 and 2007 image data sets.

### 2.6.2. Ratio Algorithm

The [19] algorithm uses a ratio of observed reflectance and two tuneable constants to derive depth ( $Z$ ) (Equation 2):

$$Z = m_1 \frac{\ln[nR_w(\lambda_i)]}{\ln[nR_w(\lambda_j)]} - m_0 \quad (2)$$

$R_w$  is the observed reflectance of the wavelength ( $\lambda$ ) for bands  $i$  and  $j$ , the ratio of which forms the basis for depth extraction (full explanation see [19]). Initially, the blue ( $\lambda_i$ ) and green ( $\lambda_j$ ) bands were used for the ratio input as they have the greatest penetration through the water column. The red band can also be used ( $\lambda_j$ ) in this ratio and was tested. The constant  $n$  is a fixed value, chosen to keep the ratio positive given any reflectance value input. The output must still be calibrated to field data to estimate actual depth. The constant  $m_1$  is most important, as it is used to tune the output of the ratio to true depth. This tuning is done manually, using field data as a guide.  $m_0$  is the offset for correction when the output should be zero (*i.e.*,  $Z = 0$ ). No special technique is required to apply this algorithm, it can be written into a simple model.

### 2.6.3. Accuracy Assessment

Accuracy was able to be assessed using the remaining field depth data that was not used for calibrating the algorithms. Scatter plots (incl.  $R^2$  and RMSE) of modelled depth vs. acoustic depth were created to quantitatively assess accuracy.

## 2.7. Seagrass Mapping

### 2.7.1. Cover Mapping Using Seagrass Percentage Cover Field Data

*Seagrass percentage cover* refers to horizontal projected foliage cover or simply the percentage of seagrass visible from birds-eye view. Seagrass percentage cover, estimated from each photograph from the transect survey field data, was directly overlaid on the image data for analysis. The overlaid seagrass data were sorted into four percentage categories—0–10%, 10–40%, 40–70%, 70–100%.

These categories were used for three main reasons; (1) they are required by local monitoring authorities, (2) recent studies in the area also used these four discrete classes and (3) [8] found that in the Eastern Banks area that only four discrete classes can be confidently separated. In addition to the above seagrass classes a *seagrass and macroalgae* class was also identified from the field data, as well as *sand* and *deep water* classes. Using the field data as a reference, polygons were drawn to digitise areas on the image that could be confidently assigned a class (*i.e.*, its seagrass percentage cover, *seagrass and macroalgae*, *sand* or *deep water*). Polygons were drawn around a group of pixels that suitably represented the benthic cover types present in the field data. As each polygon was drawn it was given a unique label, so a separate spectral signature could be trained for each polygon. After all the polygons were drawn and given a unique label, each is also given a class value corresponding to its benthic cover category (*i.e.*, 0–10% = 1, 10–40% = 2, 40–70% = 3, 70–100% = 4, SG&MA = 5, sand = 7, deep water = 8). In total, there were 194 and 198 polygons for 2004 and 2007 respectively and on average, 10–30 polygons were drawn for each field data transect.

In this cover mapping method each polygon is assigned for either calibration or validation purposes. A calibration polygon is one that is used to train spectral signatures from the image data to perform the supervised classification and a validation polygon is one that is used post-classification as a reference to assess accuracy. This method is still being developed, so there is no set method for choosing the ratio of the calibration/validation split. In this case, it was deemed there were enough polygons to split them evenly into calibration and validation polygons. This was achieved by sorting the polygons by area and then alternately assigning them *calibration* or *validation*, then separate calibration/validation polygon datasets are created. The polygons are sorted by area to assure a completely random division of the polygons into calibration and validation.

The calibration polygons are used to derive spectral signatures for the supervised classification based on a maximum likelihood algorithm. The calibration polygon dataset is used to extract a spectral signature from the image data, for each polygon. The signatures can then be viewed and any obviously inappropriate signatures removed. The resultant signature file is used to perform a *maximum likelihood* supervised classification. The validity of the classification output is then examined, obvious classification errors are removed and the corresponding signatures are removed, after which the supervised classification is repeated. One seagrass cover map was created for 2004 and one for 2007.

### 2.7.2. Seagrass Cover Change Detection

Change detection analysis is a standard procedure, particularly when comparing only two image dates. For the seagrass cover maps a post-classification comparison (PCC) was performed to assess change in benthic cover from 2004 to 2007. A matrix that describes class changes from 2004 to 2007, in terms of total pixels/area, was created along with a corresponding image file, for visual assessment. The matrix was created to show 10 change classes; *no change in SG cover*, *SG cover increase*, *SG cover decrease*, *SG to SG&MA (macroalgae)*, *SG&MA to SG*, *no change in SG&MA*, *sand to SG*, *SG to sand*, *deep water to SG* and *SG to deep water*. These classes were chosen as they best represent overall change in seagrass cover distribution as well as clearly showing change from a monitoring perspective. The PCC image was also coded to represent the above classes to enable a visual assessment of change.

### 2.7.3. Species Mapping Using Species Composition Field Data

The seagrass composition field data was also used to classify the images into seagrass species composition. The classification procedure followed the same method as the seagrass cover mapping; new polygons were drawn by overlaying the seagrass species data as compositional pie charts. The following seagrass species categories were identified; *Halophila ovalis*, *Cymodocea rotundata*, *Halodule uninervis*, *Halophila spinulosa*, *Syringodium isoetofolium*, *Zostera muelleri*, frequently occurring species combinations (e.g., *H. ovalis* and *Z. muelleri*), a sand and a deep water class. The polygons were digitised and divided into calibration/validation also following the same method as the cover mapping. A seagrass species composition map was created for both the 2004 and 2007 Quickbird images, using a maximum likelihood supervised classification with the following classes; 2004—*Halophila ovalis*, *Cymodocea rotundata*, *Halophila spinulosa*, *Syringodium isoetofolium*, *Zostera muelleri* and *Halodule uninervis/H. ovalis*, *H. spinulosa/H. ovalis* and *Z. muelleri/H. ovalis* species combinations; 2007—*dead seagrass*, *H. ovalis*, *C. rotundata*, *H. uninervis*, *S. isoetofolium*, *Z. muelleri* and a *H. spinulosa/H. ovalis* species combination

### 2.7.4. Accuracy Assessment

Accuracy of the classification outputs was assessed using the validation polygons. The validation polygon dataset was modified so that the unique value of each polygon was recoded to its corresponding benthic cover category class (e.g., every polygon in the 0–10% seagrass cover category is recoded to a value of 1, every polygon in the 10–40% seagrass cover category is recoded to a value of 2 *etc.*). This created a validation raster for each benthic cover type, which was compared to the classification outputs. The validation and classification output rasters were used to create an error matrix showing the number of pixels in the classified image that were correctly classified, according to the validation raster. From this, overall, producer and user accuracies were calculated [27] for each of the maps from both methods. Overall accuracy, including algae, sand and deepwater classes were calculated for each map as well as a “seagrass overall accuracy” that only assessed seagrass classes (*i.e.*, excluded algae, sand and deep water classes). Producer accuracy (omission error) and user accuracy (commission error) were calculated for each individual mapping class (*i.e.*, seagrass cover/species class, algae class, sand and deepwater) for each map produced. The accuracy types used above are all standard methods used to evaluate maps derived from remotely sensed data [27].

## 3. Results and Discussion

### 3.1. Bathymetry Mapping

As discussed in the methodology section, the first stage of the bathymetry mapping was to explore the relationships between depth and the image data. Using the field bathymetry data, areas of pixels around known depth points were selected and the relationship between reflectance and depth was examined. Areas were selected over sand and high and low albedo seagrass cover. The 2004 and 2007 images showed a strong linear relationship between log transformed band pairs and water depth over sand substrate up to a depth limit. The 2004 data showed a separable relationship up to about 6–8 m

deep and the 2007 image data showed a separable relationship up to about 5–6 m deep. The distribution of seagrass reflectance had a less consistent relationship with depth. There was no linear relationship between water depth and observed reflectance over seagrass cover type. The seagrass cover type has a higher degree of internal variance; therefore in a linear relationship, variance in albedo is confused with variance in water depth. For example, in the 2004 reflectance data, 1.0 m deep seagrass with a high albedo was significantly separated from the other seagrass classes including 1.0 m seagrass with low albedo, 2.0 m low/high albedo and 3.0 m, which were inseparably grouped. The 2007 reflectance data was even less consistent, and showed no distinguishable relationship. The analysis showed that band pair reflectance for seagrass and sand bottom type becomes mixed at approximately 3 metres deep, hence separating them solely on reflectance (using Quickbird band widths) would not be possible.

### 3.1.1. Linear (Lyzenga) Algorithm

The data exploration above revealed that even after splitting the images into sand and seagrass layers it would be invalid to apply the Lyzenga bathymetry algorithm to the seagrass layer. The analysis of the 2004 and 2007 images showed that the relationship between the seagrass reflectance and water depth was simply too weak for a valid application of a Lyzenga algorithm. As such, the algorithm was only applied to the sand layer, which comprises the majority of both images anyway.

The acoustic field data is limited in the sense that it was collected for a project focused on seagrass mapping; hence there is limited distribution of sites at varying depths for plain sand substrate. As such, the field data was examined and appropriate areas of sand at specific depths were identified and small groups of pixels around these points were digitised and used in the regression analysis. The regression analysis results for both image dates were consistent and practical using this method. The 2004 regression gave an  $R^2$  value of 0.88 and the 2007 regression gave an  $R^2$  value of 0.81. The equations calculated from the regression analysis were incorporated into a model and applied to the appropriate image to produce the bathymetry maps (Figure 2).

The accuracy of the Lyzenga algorithm output for each image date was assessed with a scatter plot of the Lyzenga algorithm output versus acoustic field data (including  $R^2$  and RMSE) (Figure 3). Depth values from the Lyzenga output raster were compared to the corresponding true depth field data points. The predicted values generally fitted the field data values well, although the relative accuracy of the predicted values was lower than expected. The results from the scatter plots show an over estimation of depth in shallow areas, more accurate estimation at mid-depths and somewhat of an under estimation in deeper areas. The overall accuracies are misleading in the sense that for low and high depth ranges, accuracy is between 0.7 and 1.0 m and accuracy in the mid-depth ranges is between 0.1 and 0.3 m. This trend caused overall RMSE accuracies for the 2004 and 2007 bathymetry maps to even out at 0.78 m and 0.49 m respectively. Hogrefe and Stumpf *et al.* [17,19] showed a similar pattern of over estimation at low depths and under estimation at high depths when using a linear algorithm. This shows an inherent feature of linear depth estimation; under/over estimation of water depths at either end of the saturation spectrum. Improving the regression equation, or even model complexity, by which water depth is modelled can potentially reduce the error due to this feature. However, in this case, the improvement is probably negligible compared to the magnitude of error attributable to

**Figure 2.** Bathymetry maps produced from the 2004 (left) and 2007 (right) imagery using the Lyzenga algorithm, excluding exposed areas and seagrass (marked as green).

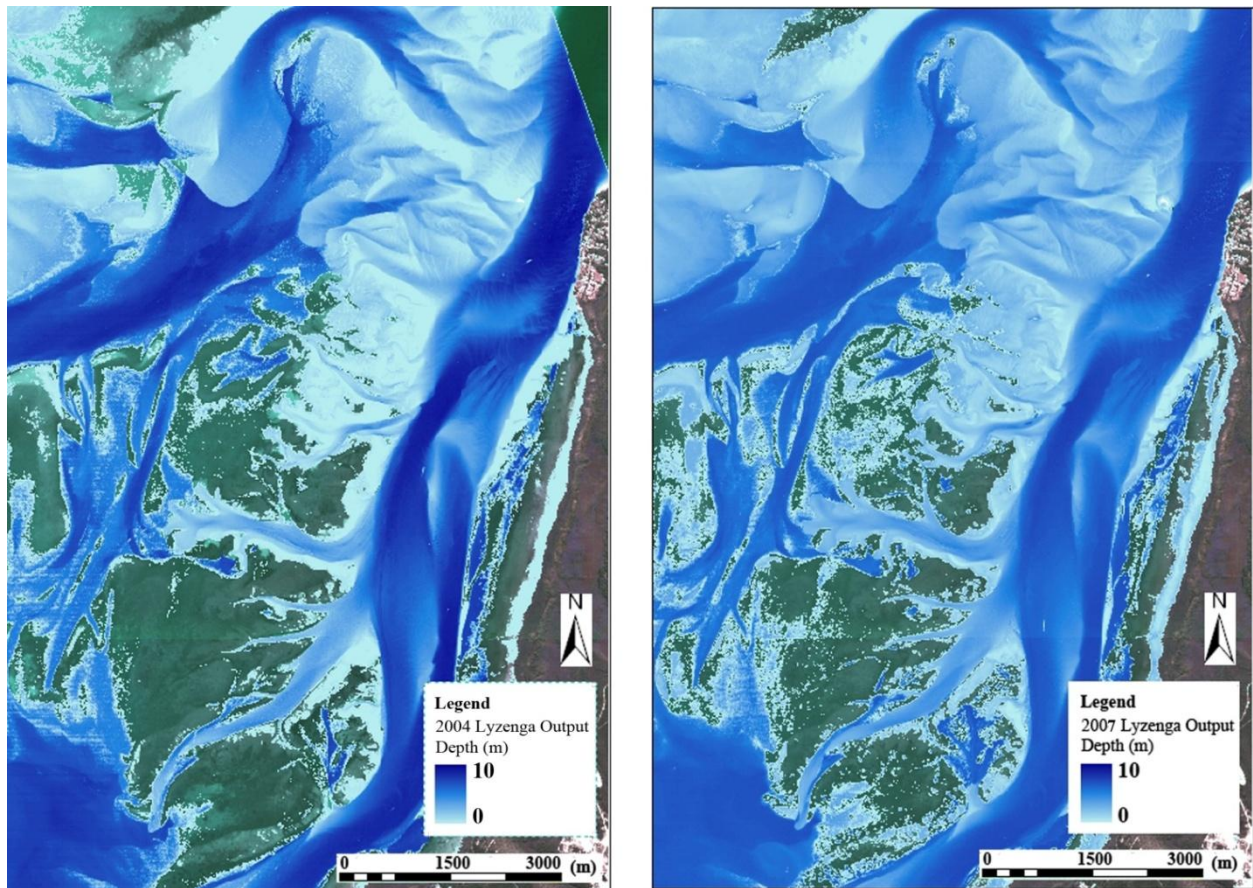
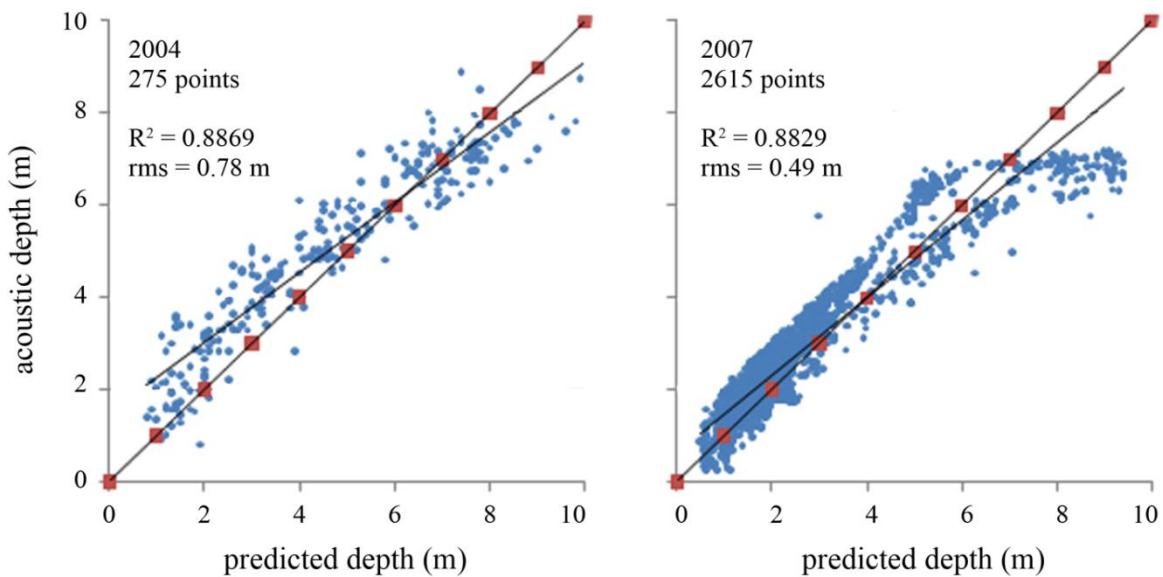


**Figure 3.** Scatter plot showing Lyzenga predicted depth vs. acoustic depth from field data points for 2004 (left) and 2007 (right) image data. Line with squares = 1:1 line; plain line = line of best fit.



unaccounted tidal variation. The field data is collected at varying tide heights opposed to the image data which is collected at a single tide height, causing error in the calibration process. The 1 m tidal

range in Moreton Bay was considered low enough to neglect tidal stage correction. This must be a consideration when using bathymetry products derived from linear (Lyzenga based) methods.

### 3.1.2. Ratio Algorithm

The exploration of the scatter plots discussed above suggested that application of the ratio algorithm would be feasible; however, this was not the case. The ratio algorithm (using blue, green and red bands) was tested on a number of different data sets, including separate and mixed seagrass and sand areas from both image dates. The reflectance ratio outputs were not varied enough to appropriately calibrate using the  $m_1$  constant. A number of different constant ( $n$ ) and transformation (including square root and other log bases) combinations were used, but this yielded no significant increases in variance. Applying the algorithm as suggested in [19] on sand substrate produced reflectance ratio outputs varying from 0.99 (at 1 m depth) to 1.05 (at 20 m depth). The output values generally increased logically from 1m to 20m but contained an unacceptable number of outliers to appropriately scale to true depth using a single scaling constant. The reason for this is not fully known, but the authors speculate that this may be caused by very low seagrass cover (<5%) that is present across much of the study site, which is practically undetectable. The results from applying the algorithm over seagrass substrate suggested that the algorithm could not take into account varying albedo over seagrass substrate, similarly to the Lyzenga algorithm. The outputs from the seagrass data sets varied from 0.97 to 1.05 almost randomly, from water depths of 0.6 m to 5 m deep, which made scaling to true depth impossible.

The poor results from this algorithm may be a reflection of the inherent challenges with empirical approaches. Although this algorithm has been shown to work in other studies [17], empirical algorithms are often site/environment specific and do not work over all substrates and water column inherent optical properties/constituent concentrations. The most likely factor for the overall failure of the ratio algorithm is the environmental differences between the Eastern Banks and the coral reef environment, where the algorithm was developed. This is partially confirmed by unpublished bathymetry mapping work (by the authors), where the algorithm was applied to a 2007 Quickbird image of Heron Reef, Australia. Areas of varying substrate and known depth had already been identified from separate research, so the algorithm was applied to these areas. Applying the algorithm produced reflectance ratio outputs with a strong correlation to depth and with further calibration could confidently estimate depth. Hogrefe *et al.* [17] also successfully used the ratio algorithm to derive water depths in a coral reef environment, suggesting that the algorithm is not suited to the Eastern Banks.

Both of the algorithms tested were not suitable over seagrass, which can be explained. Reflectance over seagrass appears to be determined by the composition and structure of the canopy and the ratio of visible sand:seagrass. Adding complexity, this ratio does not always change proportionately to horizontal percentage cover, but can also change due to water currents (effects water column constituents and canopy movement), sun angle and canopy structure/form. This ultimately causes variance in reflectance over similar levels of cover or composition to be more dependent on “environmental state” than on depth; breaking the fundamental assumption on which linear algorithms are based, that they rely on uniform, similarly behaving bottom types. This issue was not explored any

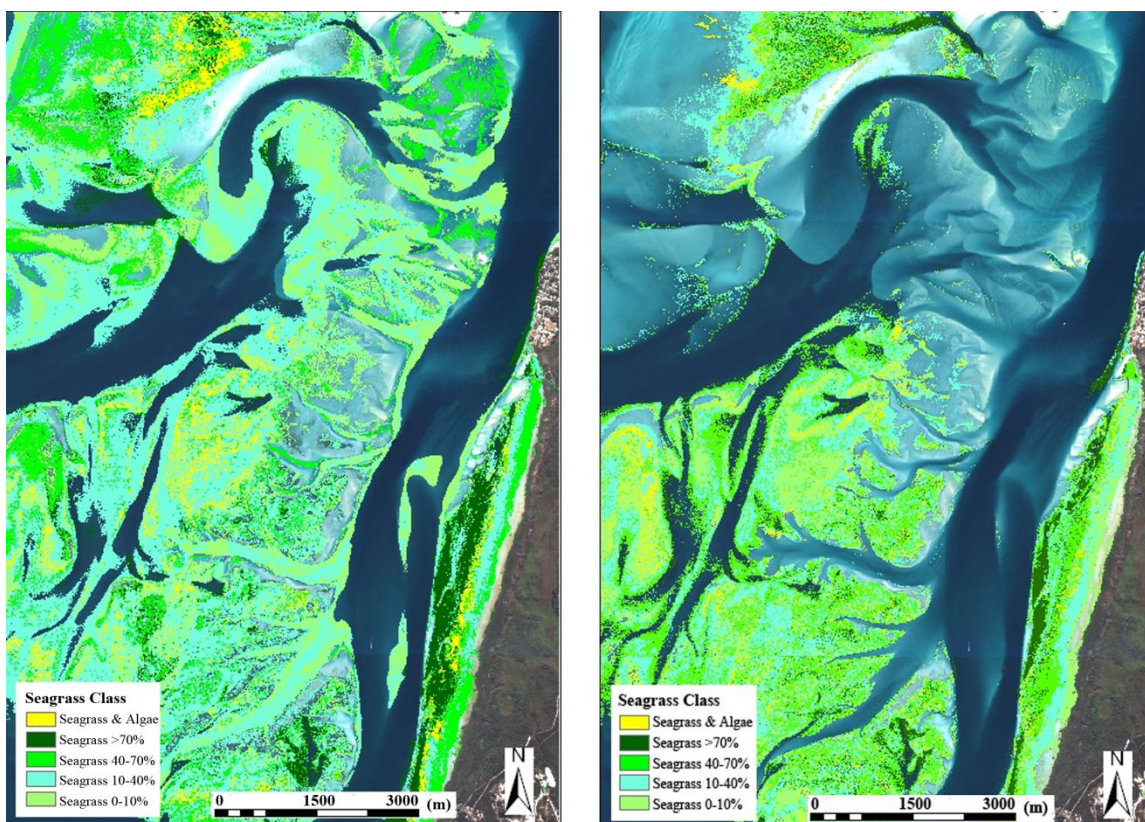
further here, but is worth consideration for future work, suggesting an algorithm that uses reflectance information to estimate cover/composition and model radiative transfer, as done in [28], would be most suitable for bathymetry mapping in Moreton Bay.

### 3.2. Seagrass Mapping

#### 3.2.1. Seagrass Cover Maps

The seagrass cover map for 2004 and 2007 showed similar outputs in terms of seagrass cover trends and also showed similar patterns of spatial distribution and cover variability to recent studies [8,9,14,16]. There are no published maps from 2005 to 2008 that are directly comparable (in terms of spatial resolution and coverage) to the 2007 seagrass cover map produced in this study. However the EHMP 2006–2007 technical report for the Eastern Banks suggested, based on field observations, minimal change in seagrass distributions and densities during this period [29]. Figure 4 shows the 2004 and 2007 seagrass cover maps produced in this study.

**Figure 4.** Seagrass percentage cover map produced for 2004 (left) and 2007 (right).



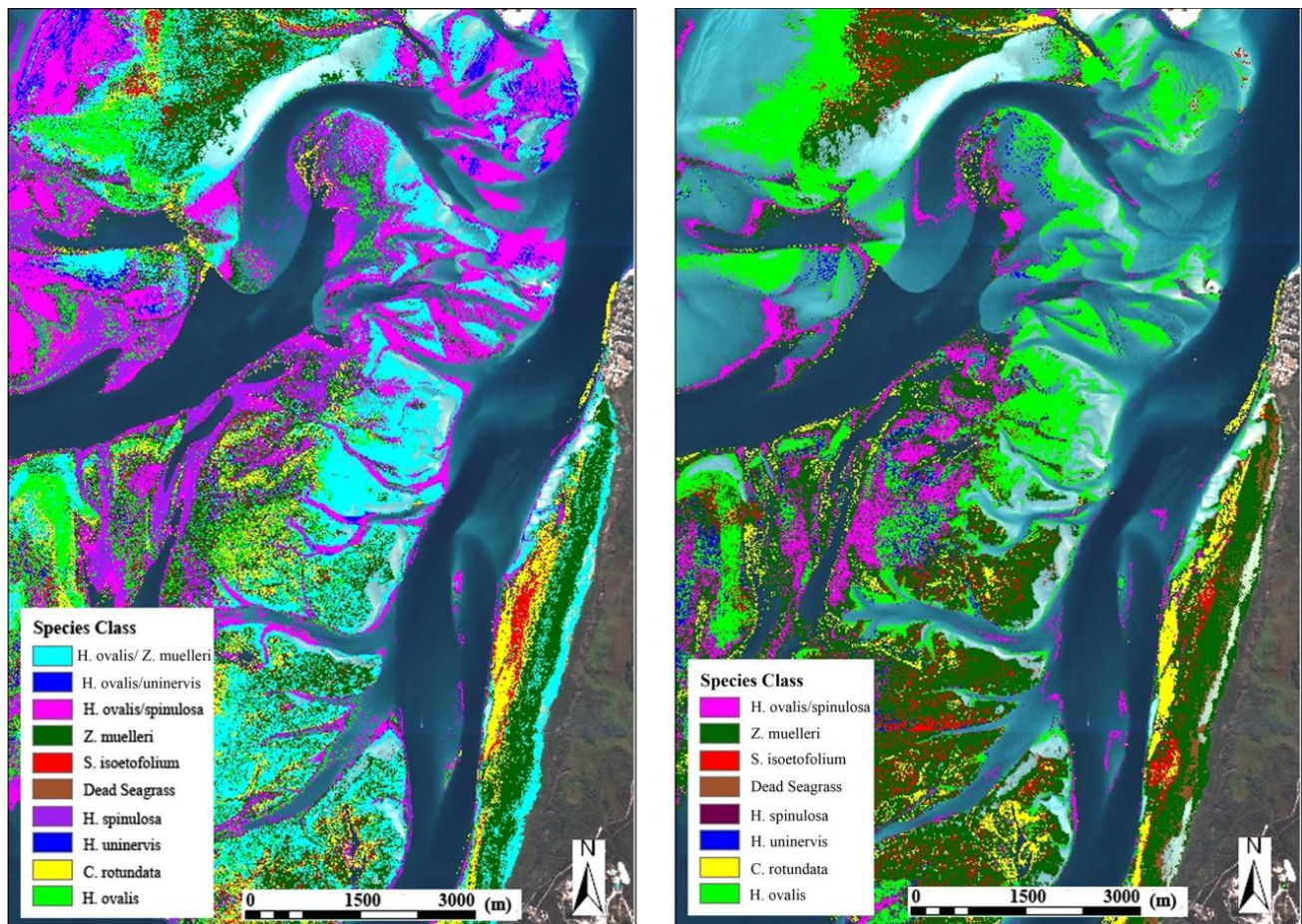
Trends in the field data are generally well represented in the classified images—both close to the field data points and between the transect locations. Consistency close to the calibration points is a function of the mapping method but consistency in areas between the field data transects is a more reliable indication of the robustness of the mapping method to correctly classify seagrass cover in areas without *in situ* field data. There are several regions on both the 2004 and 2007 maps that are identifiable by similar benthic cover patterns. The most obvious is the seagrass distribution over the

Wanga Wallen Banks (see Figure 1). The western side of the banks is dominated by high cover (>70%) seagrass and moving east the benthic cover is dominated by medium to low (10–70%) seagrass, with a defined “strip” of *seagrass and macroalgae* cover. This region of denser seagrass and macroalgae presence is due to the Wanga Wallen Banks being sheltered (by North Stradbroke Island) from tidal flushing. A similar region of high seagrass cover can also be identified in the Moreton Banks, sheltered by the southern tip of Moreton Island. The Maroom and northern Amity Banks are dominated by low cover (<40%) seagrass, although no specific pattern within the 0–10% and 10–40% classes is observable between the two image dates. The southern Amity banks, for both image dates, contain a more diverse mix of seagrass cover levels, with no obvious patterns identifiable between the two dates. It is difficult to attribute the variance in cover levels between 2004 and 2007 to either the mapping process or true changes in cover level. However, the consistent areas of seagrass cover (Moreton and Wanga Wallen banks) at least, are an argument to suggest that the mapping method is consistent.

### 3.2.2. Seagrass Species Maps

A seagrass species composition map was created for 2004 and 2007 (Figure 5). The species identified in this study are consistent with recent [8,9,16] and older [6,15] studies. The spatial distribution of species identified in this study is also consistent with [8]; the distribution of *H. ovalis* and *Z. muelleri* across most of the Amity Banks, the presence of *H. spinulosa* along channel edges and in the southern parts of the Amity Banks and the pattern of *Z. muelleri*, *C. rotundata* and *S. Isoetofolium* along the Wanga Wallen banks.

The agreement between the species field data and the species classes mapped by the classification varies across the extent of the species maps. This may be due to a lower variability between seagrass species classes compared to seagrass cover classes (*i.e.*, there is a more defined variability between low and high cover classes compared to two species classes at the same cover level). The Wanga Wallen and Moreton Banks show a high level of agreement with the field data, due to the larger areas of continuous, higher cover, homogenous species compositions. The Maroom and Amity Banks generally have poor consistency with the field data, which considerably effects the accuracy. Comparing the two maps, the 2004 and 2007 maps show a similar distribution of seagrass species and similarly to the seagrass cover maps, consistent spatial patterns can be identified between the two image dates. In both image dates the Wanga Wallen banks are defined by elongated mono-specific *strips* of *C. rotundata* and *Z. muelleri* and mono-specific areas of *S. isoetofolium*. In a specific case, the 2007 species map identified small 10–30m radial patches of *C. rotundata*, which were not mapped accurately in the 2004 species map, and have not previously been able to be mapped effectively in published work over the Eastern Banks.

**Figure 5.** Seagrass species composition map produced for 2004 (left) and 2007 (right).

In terms of specific mapping classes, there is little consistency between the two dates over the Maroom, Moreton and Amity banks. However, a pattern that is consistent across much of the Eastern Banks is that areas mapped as species combination classes in the 2004 map are often mapped as a mono-specific species class in the 2007 map (as either one of the species class from the 2004 combination). This is most prevalent with the *Z. muelleri*/*H. ovalis* combination in the 2004 map, which often corresponds to mono-specific areas of either *Z. muelleri* or *H. ovalis* in the 2007 map. There are two possible implications of this; (1) it represents a shift from a species combination to dominance by one seagrass species (ie areas of *Z. muelleri*/*H. ovalis* changed to areas of mono-specific *Z. muelleri*) or (2) comparable sites may have been incorrectly represented as mono-specific by the 2007 field data or as a species combination in the 2004 data. From the 2007 field data only one species combination was separable (*H. spinulosa*/*H. ovalis*) and no *Z. muelleri*/*H. ovalis* class was separable. A *Z. muelleri*/*H. ovalis* class was clearly separable (and abundant) in the 2004 field data and as such, large areas were identified. Therefore the observed changes from combination to mono-specific seagrass reflect distribution observed from the field data. Thus, the uncertainty is not in the map accuracy but in the way the field data is presented. If the reduction in observable species combinations in the 2007 field data are indeed a true representation, then so is the species map.

### 3.2.3. Accuracy Assessment of Seagrass Cover and Species Maps

Figures 6–8 show the accuracy level summaries for the seagrass maps produced and discussed above. In Figures 4 and 5, the *sand* and *deepwater* classes were not displayed as the focus of this paper is on the seagrass, however the accuracy of sand and deepwater were included in the accuracy summary graphs to demonstrate how high accuracies for individual classes (e.g., sand and deepwater) could boost overall accuracy. It is important to realise that these accuracy levels are not solely a reflection of map accuracy, but also reflect image data accuracy and field data consistency, in terms of both spatial accuracy and interpretation accuracy.

**Figure 6.** Accuracy values for the 2004 and 2007 seagrass cover (**left**) and seagrass species (**right**) maps. “Overall” accuracy includes all mapping classes and “Seagrass Overall” includes only the seagrass mapping categories (*i.e.*, excluding sand and deep water).

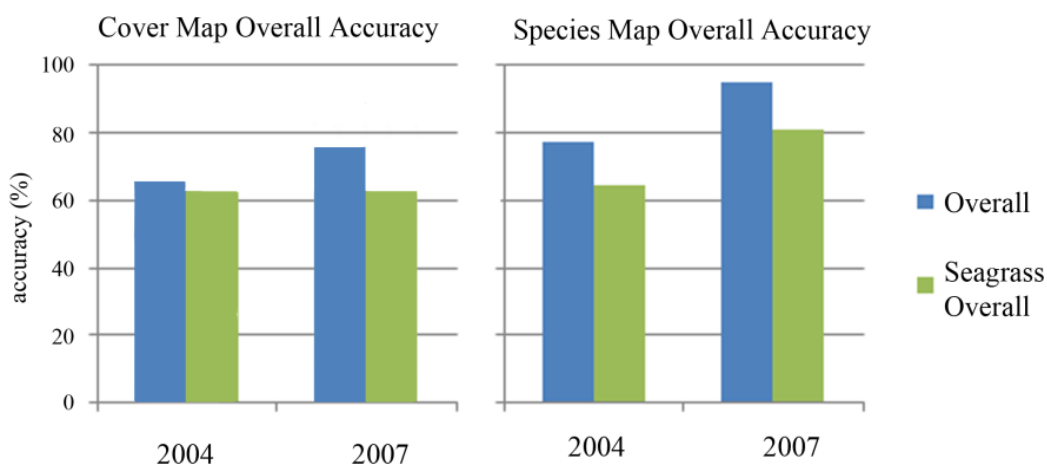


**Figure 7.** User (**left**) and Producer (**right**) accuracy values for the 2004 and 2007 seagrass cover maps. Note high accuracy values for sand and deep classes, which explains the difference between “overall” and “seagrass overall” accuracies in Figure 6.

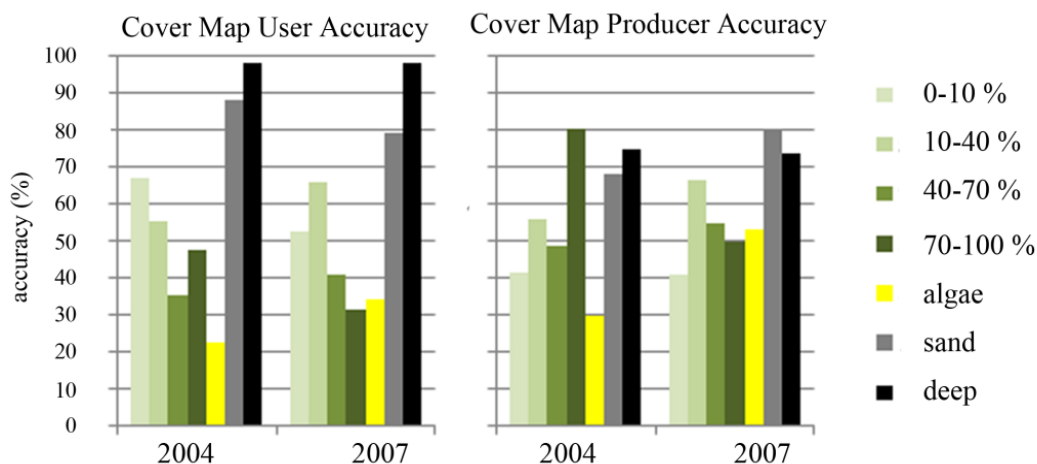
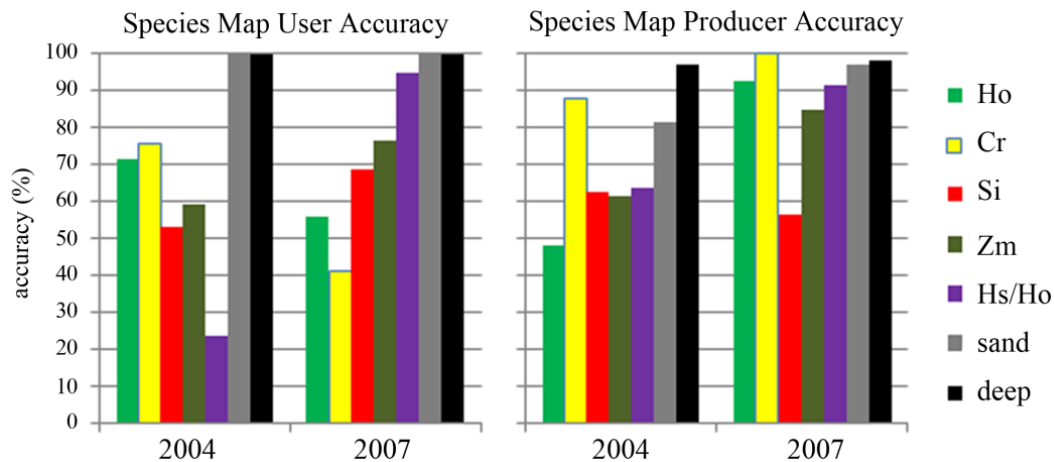


**Figure 8.** User (left) and Producer (right) accuracy values for the 2004 and 2007 seagrass species maps. Legend abbr. *Ho* = *Halophila ovalis*, *Cr* = *Cymodocea rotundata*, *Hs* = *Halophila spinulosa*, *Si* = *Syringodium isoetofolium*, *Zm* = *Zostera muelleri*.



An obvious trend in mapping accuracy is the increase in overall accuracy between 2004 and 2007, in both the cover and species maps. The increase is subtle for the seagrass cover maps but quite substantial for the species maps. An increase in accuracy between 2004 and 2007 (mapping seagrass cover) was also observed in separate seagrass mapping work by the authors (unpublished), using the same image and field data sets (making the accuracy increase unlikely to be from human error). This increase in accuracy was attributed to three possible differences in the methods for the 2004 and 2007 classifications, although they are speculative and require further research:

1. Differences in the image data, as it is possible that physical differences in atmospheric and air-water interface conditions or differences in pre-processing (particularly atmospheric correction) resulted in the 2007 image data variance, to some degree, being more suited to separating the discrete seagrass classes, resulting in a higher map accuracy.
2. Differences in tidal stage, as the tide is approximately 0.6 m lower in the 2007 image, which cannot be explicitly accounted for by corrections. As a result the 2007 image data may be more suitable to separating cover type and cause less confusion between cover types.
3. Difference in field data transect collection methods, as the 2004 field data was collected along many short transects with a high spatial coverage of the mapping extent, compared to the 2007 field data, which was collected along several longer transects with a lower spatial coverage of the mapping extent.

The seagrass cover maps reported high commission and omission error between all of the seagrass cover categories. This is consistent with findings from [8], where mapping capabilities were tested for Quickbird-2, CASI-2 and Landsat data, that the Quickbird sensor was not particularly suited to mapping discrete seagrass cover classes due to its wide spectral band range. The 0–10% cover category had the highest omission error over all of the cover maps. This was attributed mostly to confusion with the 10–40% cover class, as well as confusion with sand. Actual ground variation in seagrass cover is obviously continuous, which is the main problem with mapping discrete percentage classes—areas close to class boundaries are easily misclassified. The 70–100% seagrass cover class

was most accurately mapped, with low omission error across all of the cover maps. However, in terms of user accuracy, the trend in producer accuracy was reversed. The 0–10% cover class had the highest probability of being represented correctly on the map and the 70–100% cover class had the lowest probability. Although the 0–10% cover class was mapped poorly, due to low commission error, it is less likely on the actual map to have included an erroneous class; and vice versa for the 70–100% class. The reason for high commission error in the 70–100% cover class is attributed to its similarity to deep water and the 40–70% cover class. This again highlights the problem with mapping discrete classes over continuous attributes, as areas close to the boundary of the class have a high chance of being included in the wrong class. Based on these results, future research will focus on estimating seagrass cover as a continuous variable, rather than in discrete classes.

The accuracy trends were less consistent within the seagrass species composition maps, in relation to each other as well as compared to the seagrass cover maps. The accuracy levels reported for the 2004 species map are reasonable, but the accuracy levels for the 2007 species map appear anomalously high, compared to the 2004/2007 cover and 2004 species maps produced as well as results from published seagrass mapping studies. This anomalously high accuracy is attributed mainly to the way the field data is converted to polygons. Despite the high accuracies across both species maps, as discussed earlier, they do not consistently agree with the field data. This is believed to be responsible for the lack of relationships between omission and commission error distribution between the seagrass species classes for both species maps. At this stage, it is inappropriate to make conclusions relating to the mapping accuracy of each individual species class; in terms of which classes were erroneously included or excluded in the species map classes. Future work will involve examining species mapping further in relation to both how species classes are chosen from field data and the omission/commission error relationships between specific species classes.

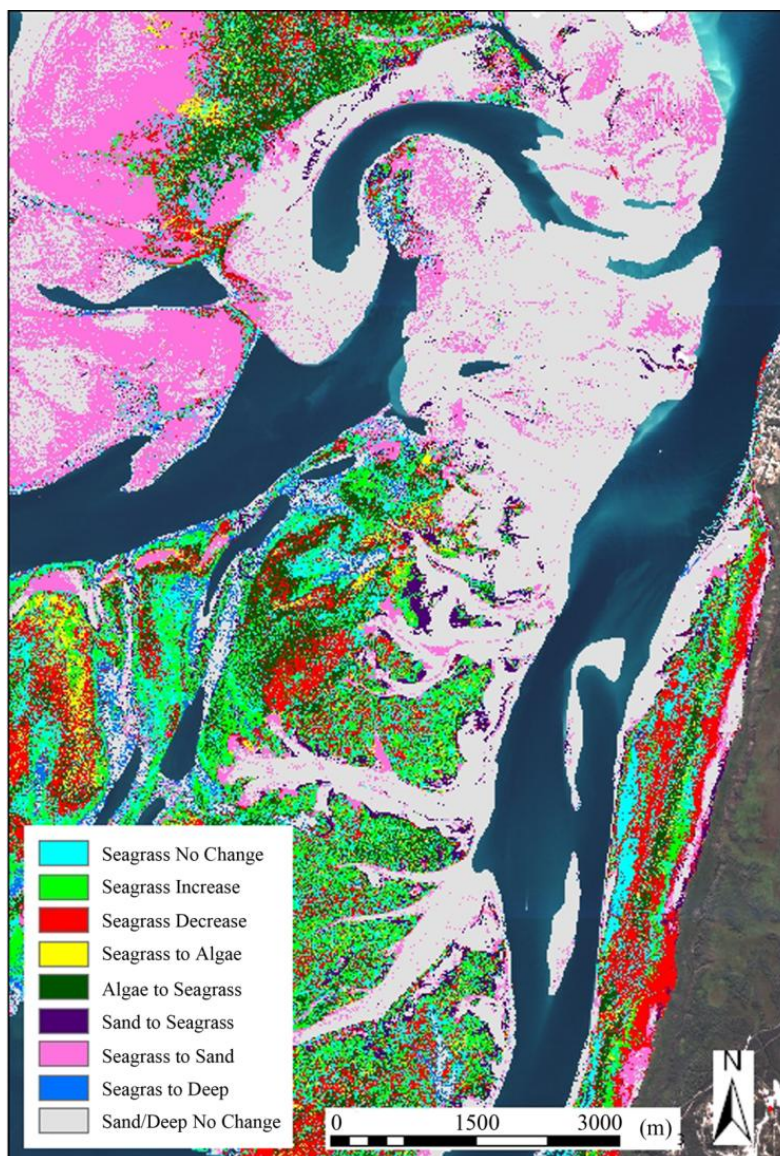
#### 3.2.4. Seagrass Cover Change Detection

Figure 9 and Table 2 show the change detection change matrix and map produced as discussed in the methodology section. In this circumstance, the only appropriate method to assign an accuracy level to the PCC image is to multiply the overall accuracy from each map used in the PCC analysis; which calculates to 49.67% ( $\approx 72\% \times 68\%$ ). This means there is approximately a 0.5 probability that change shown by the PCC image is true, which is reasonable for making generalised observations, in mapping terms. As such, it was concluded that this change assessment could only be used to make conclusions about broad scale changes in seagrass cover distribution from 2004 to 2007. If a significant change is observed over a large area, providing it is contextually reasonable, it is reasonable to assume that the change did occur between 2004 and 2007. This PCC image can provide information that has previously not been available at this resolution in a spatially continuous manner.

Overall, the change detection shows a net decrease in seagrass cover levels, but not overwhelmingly, as a much larger proportion of seagrass was shown to have not changed in cover level. The main areas of cover decrease were along the Wanga Wallen banks close to the shoreline and a large area across the western areas of the Maroom Banks. Most of these areas decreased from 10–70% cover to 0–10% cover levels. The decrease in the Wanga Wallen Banks could possibly be associated with changes in runoff patterns (incl. sediment and nutrient loads) from North Stradbroke

Island. The Wanga Wallen Banks follow the western coast of North Stradbroke Island and several creeks run directly into the banks, including a large discharge from Myora Springs. The catchment area for these creeks include several roads, urban areas and mine sites, all of which have the potential to impact on seagrass distribution, accentuated by the Wanga Wallen Banks being sheltered by the island from tidal flushing. Although the change has shown to be real and present [30], the reasons are speculative only. Areas of increased seagrass cover appear to be evenly spread across the Eastern Banks area. Large areas in the northern Eastern Banks are shown to have changed from seagrass to sand; however, this is mostly due to misclassification of sand as low cover seagrass in the 2004 cover map, again supported by [30]. This study is not concentrating specifically on ecological processes associated with seagrass change, but with further research, this study can potentially make significant improvements in understanding of how distribution in seagrass cover levels change.

**Figure 9.** Post classification change image, showing changes in seagrass cover level or substrate type from 2004 to 2007.



**Table 2.** Post classification change matrix quantifying change in cover classes as percentage of total image area, between the 2004 and 2007 seagrass cover maps. *Pale yellow = no change in SG cover, light green = SG cover increase, red = SG cover decrease, yellow = SG to SG&MA (macroalgae), dark green = SG&MA to SG, cyan = no change in SG&MA, light blue = sand to SG, light orange = SG to sand, dark blue = deep water to SG, orange = SG to deep water and grey = no change in deep water/sand.*

Numbers equal percentage (%) of total image area	2004						
	SG 0–10%	SG 10–40%	SG 40–70%	SG 70–100%	SG&MA	SAND	DEEP
<b>2007</b> SG 0–10%	1.03177	5.400157	2.08834	0.333111	1.585643	0.809072	0.003379
SG 10–40%	2.329904	7.137612	3.29067	0.89434	2.565081	1.265136	0.071463
SG 40–70%	1.194129	5.426235	3.164758	1.479492	2.155099	0.699614	0.311642
SG 70–100%	0.060584	0.468454	0.715281	1.336465	0.530358	0.047871	0.383671
SG&MA	0.453855	1.03178	0.604307	0.22009	0.589126	0.190932	0.00113
SAND	2.907038	7.097542	4.668984	0.388433	0.391735	29.42145	0.830826
DEEP	0.015427	0.4878	0.853162	0.629457	0.003095	0.537121	1.897379

### 3.2.5. Species Composition Change Detection

Improvement to the species mapping techniques in this study would allow for a similar PCC analysis for quantifying changes in species distribution. Some seagrass species grow in patterns of concentrated local growth (often spherical) whilst others spread in a more sparse and random pattern [1]. Improved techniques for seagrass species mapping would benefit the understanding of growth patterns and dynamics of individual seagrass species. This study did not focus on individual species growth, but an example of a specific species is given for *Cymodocea rotundata*, which is less tolerant to physical disturbances (particularly low light levels) than other seagrass species. Growth patterns of *C. rotundata* patches could be monitored if this species could be consistently and accurately mapped. In the 2007 species map, in the lower parts of the Amity Banks there is a large area characterised by high density, spherical *C. rotundata* patches. These patches, whilst still present, are not consistently mapped in the 2004 species map, making monitoring and comparison difficult. If these patches could be accurately and consistently mapped in the 2004 imagery, specific changes and growth of *C. rotundata* could be monitored, and potentially linked to local or large scale disturbances. There are other examples where particular species are not mapped consistently from 2004 to 2007, demonstrating that development of methods to more accurately map seagrass species is crucial, and should be a focus of future research.

## 4. Conclusions

### 4.1. Bathymetry Mapping

Exploration of the image data showed a strong relationship between observed reflectance and water depth over the sand substrate type, but revealed that no such relationship occurred for seagrass

substrate types. Reflectance over seagrass is influenced more by variance in cover type/composition than variation in water column depth; an important consideration when mapping bathymetry. The Lyzenga algorithm was effectively used to map water depth over the sand substrate type, but it was found that this algorithm could not be used to derive depth over seagrass substrate types. An algorithm based on reflectance band ratios was also tested separately on sand and seagrass substrate types. The algorithm was not able to effectively derive water depth on either substrate type (in standard form) and the results showed that a method incorporating more site-specific information would be needed.

#### 4.2. Seagrass Mapping

Seagrass percentage cover maps were produced successfully for each image data set, at accuracies as good as, or greater than previous and recent studies. The seagrass cover maps displayed a good relationship with the field data and produced a distribution consistent with historical and recent studies. A change detection analysis was also performed on the seagrass cover maps, which enabled an evaluation of broad scale changes in seagrass cover distribution across the Eastern Banks from 2004 to 2007. Change detection at this resolution and in a spatially continuous manner has not been previously performed in Moreton Bay. Seagrass species composition maps were also created for each image data set and provided maps of seagrass species distribution at a higher resolution and spatial continuity than almost all previous studies in Moreton Bay. The validation results for the species maps was considered to be too inconsistent to enable confident conclusions about changes in species distribution from 2004 to 2007, but there were enough examples to show that monitoring changes in seagrass species distribution would be possible and also beneficial. Overall, the seagrass percentage cover maps and the seagrass species maps present significant progress to current benthic habitat mapping approaches, not only in the Eastern Banks of Moreton Bay but for a wider application to similar coastal environments.

#### 4.3. Final Remarks

Spatially extensive data has become critical for monitoring, mapping, modelling and management applications. The methods used and developed in this study offer a generation of ecologically significant information at a resolution and spatial distribution significantly higher than historical and recent studies. Moreover, the bathymetry and seagrass products for each year were produced from a single remotely sensed data set, which should provide encouragement to management agencies for investing in the use of remote sensing as a mapping, monitoring and management tool.

#### Acknowledgements

The authors would like to acknowledge staff, students and volunteers from UQ, Moreton Bay Research Station, UniDive, Seagrass Watch, Port of Brisbane, the Queensland Department of Environment and Resource Management, and the Ecological Health and Monitoring Program for help with collection and processing of field data. Authors would also like to thank the two anonymous reviewers whose comments were detailed and constructive, improving the overall quality of the paper. Authors would also like to acknowledge funding sources provided by the CRC for Coastal Zone, Estuaries and Waterways Management and an ARC Linkage LP0214956 grant to J. Marshall and S.

Phinn (Vision and remote sensing: using nature's technology to examine the health of The Great Barrier Reef and Moreton Bay).

## References and Notes

1. Larkum, A.; Orth, R.; Duarte, C.M. *Seagrasses: Biology, Ecology and Conservation*; Springer: Dordrecht, The Netherlands, 2006.
2. Frost, M.T.; Rowden, A.A.; Attrill, M.J. Effect of habitat fragmentation on the macroinvertebrate infaunal communities associated with the seagrass *Zostera marina* L. *Aquat. Conserv. Marine Freshwater Ecosyst.* **1999**, *9*, 255-263.
3. Short, F.; Coles, R. *Global Seagrass Research Methods*; Elsevier: Amsterdam, The Netherlands, 2001.
4. Green, E.P.; Mumby, P.J.; Edwards, A.J.; Clark, C.D. *Remote Sensing Handbook for Tropical Coastal Management*; UNESCO: Paris, France, 2000.
5. Dekker, A.G.; Brando, V.; Anstee, J. Retrospective seagrass change detection in a shallow coastal tidal Australian lake. *Remote Sens. Environ.* **2005**, *97*, 415-433.
6. Dierssen, H.M.; Zimmerman, R.C.; Leathers, R.A.; Downes, T.V.; Davis, C.O. Ocean color remote sensing of seagrass and bathymetry in the Bahamas Banks by high-resolution airborne imagery. *Limnol. Oceanogr.* **2003**, *48*, 444-455.
7. McKenzie, L.; Finkbeiner, M.; Kirkman, H. Seagrass mapping methods. In *Global Seagrass Research Methods*; Short, F., Coles, R., Eds.; Elsevier: Amsterdam, The Netherlands, 2001.
8. Phinn, S.; Roelfsema, C.; Dekker, A.; Brando, V.; Anstee, J. Mapping seagrass species, cover and biomass in shallow waters: An assessment of satellite multi-spectral and airborne hyper-spectral imaging systems in Moreton Bay (Australia). *Remote Sens. Environ.* **2008**, *112*, 3413-3425.
9. Roelfsema, C.M.; Phinn, S.R.; Udy, N.; Maxwell, P. An Integrated Field and Remote Sensing Approach for Mapping Seagrass Cover, Moreton Bay, Australia. *J. Spatial Sci.* **2009**, *54*, 45-62.
10. Armstrong, R.A. Remote sensing of submerged vegetation canopies for biomass estimation. *Int. J. Remote Sens.* **1993**, *14*, 10-16.
11. Benfield, S.L.; Guzman, H.M.; Mair, J.M.; Young, J.A.T. Mapping the distribution of coral reefs and associated sublittoral habitats in Pacific Panama: A comparison of optical satellite sensors and classification methodologies. *Int. J. Remote Sens.* **2007**, *28*, 5047-5070.
12. Fyfe, S.K. Spatial and temporal variation in spectral reflectance: Are seagrass species spectrally distinct? *Limnol. Oceanogr.* **2003**, *48*, 464-479.
13. Mumby, P.J.; Green, E.P.; Edwards, A.J.; Clark, C.D. The cost-effectiveness of remote sensing for tropical coastal resources assessment and management. *J. Environ. Manage.* **1999**, *55*, 157-166.
14. Dennison, W.C.; Abal, E.G. *Moreton Bay Study: A Scientific Basis for the Healthy Waterways Campaign*; South East Qld Regional Water Quality Management Strategy Team: Brisbane, QLD, Australia, 1999.
15. Hyland, S.J.; Courtney, A.F.; Butler, C.J. *Distribution of Seagrass in the Moreton Region from Coolangatta to Noosa*; Queensland Department of Primary Industries: Brisbane, QLD, Australia, 1989.

16. Zharikov, Y.; Skilleter, G.; Loneragan, N.; Taranto, T.; Cameron, B. Mapping and characterising subtropical estuarine landscapes using aerial photography and GIS for potential application in wildlife conservation and management. *Biol. Conserv.* **2005**, *125*, 87-100.
17. Hogrefe, K.; Wright, D.; Hochberg, E.J. Derivation and integration of shallow-water bathymetry: Implications for coastal terrain modeling and subsequent analyses. *Marine Geodesy* **2008**, *31*, 299-317.
18. Mumby, P.J.; Clark, C.D.; Green, E.P.; Edwards, A.J. Benefits of water column correction and contextual editing for mapping coral reefs. *Int. J. Remote Sens.* **1998**, *19*, 203-210.
19. Stumpf, R.P.; Holderied, K.; Sinclair, M. Determination of water depth with high-resolution satellite imagery over variable bottom types. *Limnol. Oceanogr.* **2003**, *48*, 547-556.
20. Lyzenga, D.R. Passive remote sensing techniques for mapping water depth and bottom features. *Appl. Opt.* **1978**, *17*, 379-383.
21. Van Hengel, W.; Spitzer, D. Multi-temporal water depth mapping by means of Landsat TM. *Int. J. Remote Sens.* **1991**, *12*, 703-712.
22. Roelfsema, C.M.; Joyce, K.E.; Phinn, S.R. Evaluation of benthic survey techniques for validating remotely sensed images of coral reefs. In *Proceedings of 12th International Coral Reefs Symposium*, Okinawa, Japan, 2004; International Coral Reef Society: Okinawa, Japan, 2004.
23. Brando, V.; Dekker, A.G. Satellite hyperspectral remote sensing for estimating estuarine and coastal water quality. *IEEE Trans. Geosci. Remote Sens.* **2003**, *41*, 1378-1387.
24. Phinn, S.R.; Dekker, A.G.; Brando, V.; Roelfsema, C. Mapping water quality and substrate cover in optically complex coastal and reef waters: An integrated approach. *Marine Pollut. Bull.* **2005**, *51*, 459-469.
25. Green, E.P.; Edwards, A.J.; Mumby, P.J. Mapping bathymetry. In *Remote Sensing Handbook for Tropical Coastal Management*; Edwards, A.J., Ed.; UNESCO: Paris, France, 2000.
26. Philpot, W.D. Bathymetric mapping with passive multispectral imagery. *Appl. Opt.* **1989**, *28*, 1569-1578.
27. Congalton, R.; Green, K. Basic analysis techniques. In *Assessing the Accuracy of Remotely Sensed Data: Principles and Practices*; Congalton, R., Green, K., Eds.; CRC Press: Boca Raton, FL, USA, 1999; Chapter 5.
28. Brando, V.E.; Anstee, J.M.; Wettle, M.; Dekker, A.G.; Phinn, S.R.; Roelfsema, C. A physics based retrieval and quality assessment of bathymetry from suboptimal hyperspectral data. *Remote Sens. Environ.* **2009**, *113*, 755-770.
29. EHMP. *Ecosystem Health Monitoring Program 2006-2007 Annual Technical Report*; Moreton Bay Waterways and Catchments Partnership: Brisbane, QLD, Australia, 2008; p. 93.
30. Lyons, M.B.; Phinn, S.R.; Roelfsema, C.M. Long Term Monitoring of Seagrass Distribution in Moreton Bay, Australia, from 1972 to 2010 Using Landsat MSS, TM, ETM+. In *Proceedings of the 30th International Symposium on Geoscience and Remote Sensing*, Honolulu, HI, USA, July 25-30, 2010.